Journal of Rehabilitation in Civil Engineering 7-4 (2019) 114-133

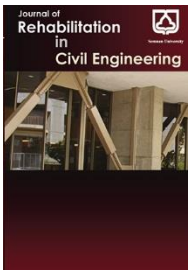

journal homepage: http://civiljournal.semnan.ac.ir/

Selection of Optimal Intensity Measure for Seismic Assessment of Steel Buckling Restrained Braced Frames under Near-Fault Ground Motions

E. Javadi[1] and M. Yakhchalian[1*]
1. Department of Civil Engineering, Qazvin Branch, Islamic Azad University, Qazvin, Iran

Corresponding author: *m.yakhchalian@qiau.ac.ir*

ARTICLE INFO

Article history:
Received: 02 June 2018
Accepted: 07 November 2018

Keywords:
Buckling Restrained Braced Frame,
Intensity Measure,
Efficiency,
Sufficiency,
Pulse-Like Near-Fault Ground Motions.

ABSTRACT

Buckling restrained braces (BRBs) have a similar behavior under compression and tension loadings. Therefore, they can be applied as a favorable lateral load resisting system for structures. In the performance-based earthquake engineering (PBEE) framework, an intermediate variable called intensity measure (IM) links the seismic hazard analysis with the structural response analyses. An optimal IM has desirable features including efficiency, sufficiency and predictability. In this paper, the efficiency and sufficiency of some traditional, cumulative-based, and advanced scalar IMs to predict maximum interstory drift ratio (MIDR) demand on low- to mid-rise steel structures with BRBs, under near-fault ground motion records having forward directivity, are investigated. The results indicate that most of the IMs contemplated are not sufficient with respect to source-to-site distance (R), for predicting MIDR. It is also demonstrated that decreasing the strain hardening ratio decreases the efficiency of the IMs. In addition, $IM_{M(\lambda=0.5)}$ and Sa_{avg} are more efficient and also sufficient with respect to pulse period (T_p), for predicting MIDR demand on the low-rise steel BRB frames under near-fault ground motions, when compared with the other IMs. In the case of mid-rise structures, PGV and $IM_{M(\lambda=0.33)}$ are selected as optimal IMs. As a result of the higher efficiency and sufficiency of the selected optimal IMs, the obtained fragility curves calculated applying these IMs, are more reliable in comparison with the fragility curves calculated using other IMs.

1. Introduction

Assessing the risk to a structure from future earthquakes requires the estimation of both the probability of occurrence of future earthquakes (seismic hazard) and the resulting structural response. Currently, non-linear dynamic analyses are being applied as a common strategy in order to evaluate the seismic demands on structures under earthquake excitations. Consequently, to have more reliable and realistic structural seismic assessments, it is necessary to

DOI: 10.22075/JRCE.2018.14908.1278

investigate the properties of ground motions that are strongly related to the structural response. According to performance-based earthquake engineering (PBEE) framework [1], an intermediate variable which links the seismic hazard and structural response analyses is termed intensity measure (IM) [2].Specifically, an IM demonstrates the strength of a ground motion and quantifies its effect on structures. The desirable features of an optimal IM are introduced as efficiency, sufficiency, and predictability [3,4]. Efficiency is the ability of an IM to predict the structural seismic response with small dispersion. In fact, efficiency of an IM express the positive interpretative power of the IM to predict the structural seismic response, and causes a reduction in the number of non-linear dynamic analyses required to achieve a given standard error [5]. The ability of an IM to render the structural response conditionally independent of the other ground motion characteristics such as magnitude (M), source-to-site distance (R), and in near-fault ground motions the period of pulse (T_p), is termed sufficiency. Predictability is defined when the IM has a reliable ground motion prediction equation (GMPE). In fact, applying an optimal IM increases the reliability of seismic performance assessments [6].

Forward directivity and fling step are two well-known phenomena which have been observed widely in pulse-like near-fault ground motions [7–10]. When the rupture propagates toward a site at a velocity close to the shear wave velocity, forward directivity occurs and causes a single large long-period two-sided pulse at the beginning of the record, which contains most of the input energy from the rupture process. Generally, the long-period pulse is expected to occur in the fault-normal direction at sites in the proximity of an active fault, where the rupture is propagating toward the site. Fling step is the permanent static displacement in the fault-parallel direction, for strike-slip faults, or in the fault-normal direction for dip-slip faults. Fling step generates a one-sided velocity pulse [11]. As mentioned by Tothong and Cornell [7], the two-sided pulse caused by the forward directivity is more damaging than the one-sided pulse caused by the fling step. Put it differently, forward directivity may lead to severe damages to buildings at near-fault regions, when compared with fling step. Many studies have been conducted in order to inquire the seismic performance of structures under near-fault ground motions (e.g., [7–11]), and most of them showed that the structural responses are significantly affected by the period of the pulse (T_p) existing in these types of ground motions.

Investigating the past earthquakes, such as 1994 Northridge and 1995 Kobe events, proved that conventional concentric braces, under seismic loading, undergone large deformations in the post-buckling range, leading to large reversed cyclic rotation at the plastic hinges formed in the brace members, and in the connections at either end [12,13]. Therefore, this type of structures suffered extensive damage, and extensive repair cost and upgrading works were needed. As an alternative, buckling restrained braces (BRBs) can be used as an effective dissipating energy system in structures. As a result of their stable tension–compression hysteretic cycles, this type of braces has been studied and experimented by many researchers in the seismic protection and retrofitting of structures [14–16].

In consonance with the definition of the optimal IM, application of an optimal IM for

seismic performance assessment of structures increases the reliability of the assessments. Hence, studies for proposing and also selecting optimal IMs for predicting different engineering demand parameters (EDPs) in different structural systems are continued (e.g., see [4–8,17–23]). It is note-worthy to mention that another method for reliable seismic performance assessment of structures is using ground motion selection methods (e.g., see [24–26]). In this research, the efficiency and sufficiency of some conventional and advanced IMs for reliable prediction of maximum interstory drift ratio (MIDR) demand, as one of the most prevalent EDPs, on steel BRB frames under near-fault ground motions having forward directivity were investigated. Subsequently, optimal IMs for reliable seismic assessment of MIDR demand on the low- to mid-rise steel BRB frames were selected.

2. Studied IMs

In this study, in order to determine the optimal IM for reliable prediction of MIDR demand on BRB frames under near-fault pulse-like ground motions, peak IMs including peak ground acceleration (PGA), peak ground velocity (PGV), peak ground displacement (PGD), as traditional IMs, were considered. In addition, pseudo spectral acceleration at the fundamental period of the structures ($Sa(T_1)$) as a traditional and the most prevalent scalar IM was taken into account. Moreover, two cumulative-based IMs that are Arias intensity (AI) [27] and cumulative absolute velocity (CAV) [28] were considered. These cumulative-based IMs are defined as follows:

$$\mathrm{AI}=\frac{\pi}{2g}\int_0^{t_f} a(t)^2 dt \quad (1)$$

$$\mathrm{CAV}=\int_0^{t_f}|a(t)|dt \quad (2)$$

where t_f is the total duration of ground motion; $a(t)$ is the ground motion acceleration at time t, and g is the acceleration of gravity. In addition to the traditional and cumulative-based IMs, five advanced scalar IMs, described in the rest of this section, were pondered. Cordova et al. [18] proposed a two-parameter power-law form scalar IM to account for the period lengthening due to non-linear deformations. They used four moment resisting frames including three composite frames (composed of reinforced concrete columns and steel beams) and one steel frame. They demonstrated that applying an elastic spectral shape indicator in addition to $Sa(T_1)$ can result in an improved IM as:

$$IM_C=Sa(T_1)\times\left[\frac{Sa(2T_1)}{Sa(T_1)}\right]^{0.5} \quad (3)$$

where $Sa(2T_1)$ is the spectral acceleration ordinate at the period two times T_1. By using a set of single degree of freedom (SDOF) systems, Mehanny [19] applied an enhanced broad-range spectral shape-based power-law form to improve IM_C, and developed a more efficient IM as follows:

$$\mathrm{IM_M}=\mathrm{Sa(T_1)}\times\left[\frac{\mathrm{Sa}(R^{\lambda}\mathrm{T_1})}{\mathrm{Sa(T_1)}}\right]^{0.5} \quad (4)$$

where λ is 0.5 or 0.33; and R is defined as the ratio of the lateral strength required to maintain the system elastic to the lateral yielding strength of system. In the present study, R was considered as:

$$R=\frac{Sa(T_1)}{g.Y} \quad (5)$$

where Y is the ratio of fully yielded strength of structure to seismic weight (V_y/W). The other well-known and advanced IM considered is I_{Np} that was proposed by

Bojórquez and Iervolino [20]. They applied a set of structures including non-linear SDOF systems, reinforced concrete and steel moment resisting frames to propose I_{Np}. This IM applies $Sa(T_1)$ and a spectral shape proxy named *Np* as:

$$I_{Np}=Sa(T_1)Np^{0.4}; \qquad Np=\frac{Sa_{avg}(T_1...T_N)}{Sa(T_1)} \qquad (6)$$

where $Sa_{avg}(T_1…T_N)$ is the geometric mean of spectral acceleration ordinates over the period range of T_1–T_N, $T_N = 2T_1$. Eads et al. [21] also applied the geometric mean of spectral acceleration ordinates over an increased period range (in comparison with I_{Np}) and proposed Sa_{avg} as a scalar IM. They deliberated nearly 700 moment resisting frame and shear wall structures. In fact, in order to consider both the higher mode and period elongation, they increased the period range. Sa_{avg} is defined as:

$$Sa_{avg} = Sa_{avg}(\alpha_1 T_1 \dots \alpha_N T_1)=$$

$$= \sqrt[N]{\prod_{j=1}^{N} Sa(\alpha_j T)} \qquad (7)$$

where α_1 and α_N are 0.2 and 3.0, respectively. In addition, Sa_{avgM} that is Sa_{avg} with a modified period range, i.e., $0.2T_1$–$\sqrt{R}T_1$, was considered. A similar form of Sa_{avgM} was studied by Jamshidiha et al. [17]. They inquired the efficiency and sufficiency of Sa_{avgM} for collapse capacity prediction of steel moment resisting frames with fluid viscous dampers. Recently, Bojórquez et al. [22] contemplated six moment-resisting steel frames to ameliorate I_{Np}, and proposed I_B, which accounts for higher mode effects. I_B is defined as:

$$I_B=S(T_1)Np^{b_1} \prod_{i=2}^{i=\#\,\text{modes}} \left[R_{T1,Tmi}^{b_2}\right]; \qquad R_{T1,Tmi}=\frac{S(T_{mi})}{S(T_1)} \qquad (8)$$

where $S(T_1)$ is a spectral parameter at T_1, taken from any type of spectrum (i.e., acceleration, velocity or displacement). T_{mi} is the period of *mode i* of vibration of the structure. Similar to Bojórquez et al. [22], in this study b_1 and b_2 were assumed equal to 0.4 and 0.2, respectively. Moreover, the pseudo acceleration response spectrum was applied to obtain $S(T_1)$ and $S(T_{mi})$, and only the second mode of vibration was considered to define $R_{T1,Tmi}$. Table 1 presents the IMs considered in this study. According to the above-mentioned explanations, it can be inferred that investigating the efficiency and sufficiency of the advanced IMs for the prediction of structural seismic response of BRB frames has not been conducted yet.

3. Structural Models

In this study, it was of interest to design three low- to mid-rise BRB frames in order to investigate the efficiency and sufficiency of the IMs for seismic assessment of this type of structures under pulse-like near-fault ground motions. The examined frames are 3-, 6-, and 9-story 2-dimentional (2D) BRB frames extracted from 3-dimentional (3D) building frames with 3.6 m stories height, and bays width of 7.5 m. All BRBs in braced bays were used in chevron configuration.

Table 1. Considered IMs.

Considered IMs	Developer
PGA	
PGV	
PGD	
$Sa(T_1)$	
AI	Arias [27]
CAV	Benjamin [28]
IM_C	Cordova et al. [18]
$IM_{M(\lambda=0.33)}$	Mehanny [19]
$IM_{M(\lambda=0.5)}$	Mehanny [19]
I_{Np}	Bojórquez and Iervolino [20]
Sa_{avg}	Eads et al. [21]
Sa_{avgM}	Jamshidiha et al. [17]
I_B	Bojórquez et al. [22]

Figure 1 presents the plan and geometry of the considered structures. The examined frames were located in a high seismic site at California with site class D according to ASCE 7-10 [29]. The seismic parameters S_s and S_1 were pondered 1.875 and 0.6, respectively; the importance factor (I) of 1, and the response modification factor (R) of 8 were considered based on ASCE 7-10 [29].

The gravity dead and live loads of 4.1 kN/m^2 and 1.5 kN/m^2, respectively, for roof, and the gravity dead and live loads of 4.1 kN/m^2 and 2.5 kN/m^2, respectively, for the other stories, were deliberated. 4.5 kN/m was applied as the dead load of curtain walls on the perimeter beams. The equivalent lateral force procedure based on ASCE 7-10 [29] and the load and resistance factors design (LRFD) load combinations of ASCE 7-10 [29] were applied for designing the structures. The specification for structural steel buildings (ANSI/AISC 360-10) [30], and seismic provisions for structural steel buildings (ANSI/AISC 341-10) [31] were applied for designing the structural elements as well. I- and H- shaped sections, with yield stress of F_y=345 MPa, were taken into account for beams and columns, respectively; and F_y=262 MPa was also contemplated for BRBs steel core. Moreover, all of the beam-to-column, column-to-base, and brace connections were assumed pinned. Table 2 depicts the fundamental periods, seismic response coefficients (C_s) and designed sections for structural members.

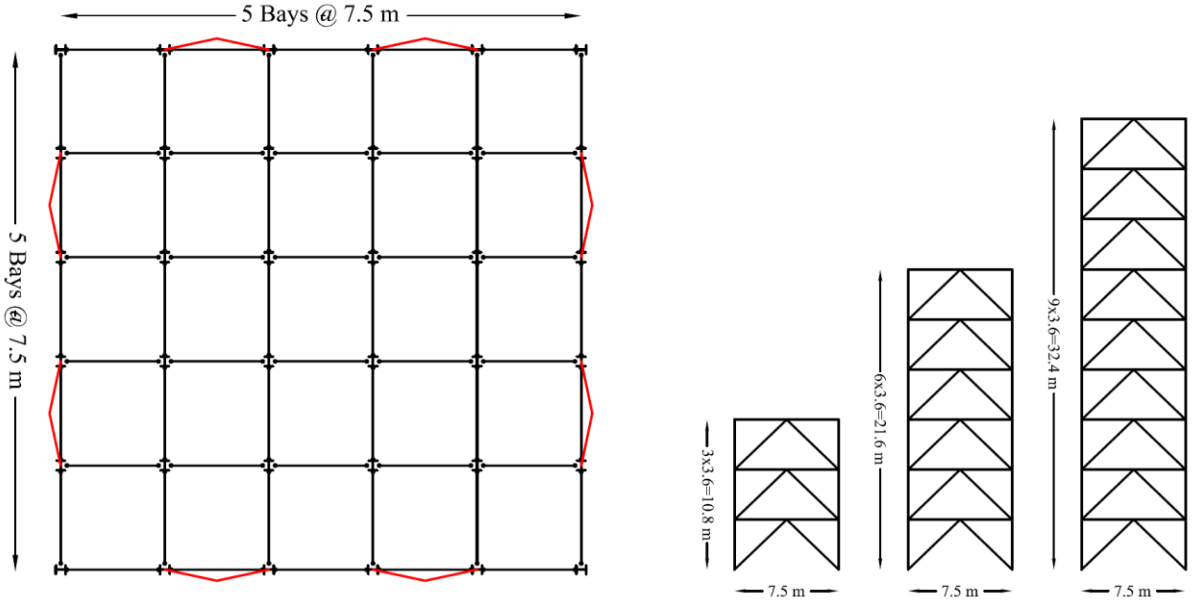

Fig. 1. (a) Plan of 3-, 6- and 9-story BRB frames, and (b) the geometry of the 2D braced bays.

4. Non-Linear Models and Dynamic Analyses

For non-linear dynamic analyses, the structural models were generated with the OpenSees [32] software. In order to model the non-linear behavior of beams, columns, and yielding segments of braces, non-linear beam–column element with five integration points, using a fiber section with Steel02 [33] material model was applied. The parameters required for Steel02 material model were extracted from the study performed by

Guerrero et al. [34], and similar to their study, cyclic degradation was neglected. 70% of each brace work-point to work-point length was considered as yielding segment. Based on the study conducted by Mahdavipour and Deylami [35], decreasing the strain hardening ratio in BRBs, increases the residual drift demands of low- and medium-rise BRB frames, and the restoring ability of BRB frames reduces meaningfully. Therefore, as a result of the substantial effects of strain hardening ratio on the seismic performance of BRB frames, two strain hardening ratios (h) of 0.003 and 0.02 were deliberated in this study for non-linear elements. The P-Δ effect was considered in analyses. In order to ponder the P-Δ effect of gravity frames, leaning column technique was devised through adding a gravity low lateral stiffness column that was linked to the main structure. Gravity loads of gravity frames were applied to the leaning column [36]. 5% Rayleigh damping was assigned to the first mode and the mode at which the cumulative mass participation exceeds 95%.

Table 2. Fundamental periods, seismic response coefficients (C_s) and designed sections for structural members.

No. of Stories	T(s)	C_s	Story No.	Sections		
				BRB	Beam	Column
3	0.543	0.156	1	Star BRB-4.5	IPE360	HE220B
			2	Star BRB-3.5	IPE330	HE220B
			3	Star BRB-2.0	IPE300	HE220B
6	1.061	0.102	1	Star BRB-5.0	IPE360	HE400B
			2	Star BRB-5.0	IPE360	HE400B
			3	Star BRB-4.5	IPE360	HE260B
			4	Star BRB-3.5	IPE360	HE260B
			5	Star BRB-2.5	IPE300	HE220B
			6	Star BRB-1.5	IPE240	HE220B
9	1.547	0.076	1	Star BRB-6.0	IPE400	HE500M
			2	Star BRB-5.5	IPE400	HE500M
			3	Star BRB-5.5	IPE400	HE500M
			4	Star BRB-5.0	IPE360	HE450B
			5	Star BRB-5.0	IPE360	HE450B
			6	Star BRB-4.0	IPE330	HE360B
			7	Star BRB-4.0	IPE330	HE360B
			8	Star BRB-3.0	IPE300	HE280B
			9	Star BRB-2.0	IPE300	HE280B

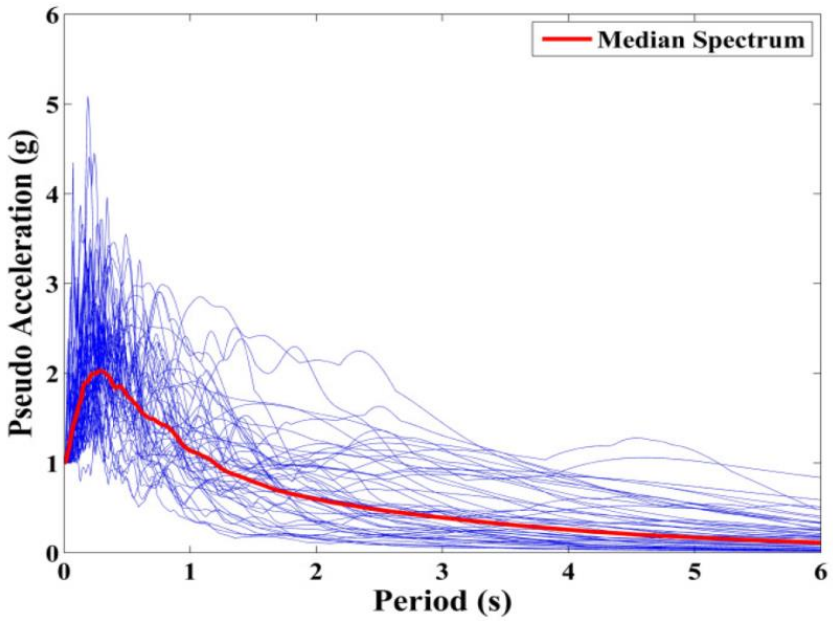

Fig. 2. Pseudo acceleration response spectra of the ground motion records (PGA=1.0g).

To perform non-linear dynamic analyses a set including 48 pulse-like near-fault ground motion records, having forward directivity effect, was applied. As a result of the forward directivity effect, these records contain a single large long-period two-sided pulse at the beginning of the record, which contains most of the input energy from the rupture process. The records have minimum useable frequencies of less than 0.2 Hz, and they were rotated to the fault-normal direction and taken from the PEER NGA database [37]. This ground motion record set was also used by Yakhchalian et al. [8]. The 5% damped normalized pseudo acceleration response spectra (PGA=1.0g) and their median spectrum are highlighted in Figure 2.

To investigate the impact of efficiency and sufficiency of the IMs, non-linear dynamic analyses were performed applying the cloud method [2]. In agreement to this method, non-linear dynamic analyses are performed by using a set of ground motion records with associated IM values. The records are not scaled, or all records are scaled by a constant factor if the unscaled records are not strong enough to lead to the structural response level of interest. Generally, the set of IM values and the associated EDP values, obtained from the non-linear dynamic analyses, are similar to a rough ellipse and called cloud (e.g., see Figure 3). A regression can be applied to this cloud of data to calculate the conditional mean and standard deviation of ln*EDP* given IM as:

$$\ln EDP = a_0 + a_1 \ln IM + e \tag{9}$$

where a_0 and a_1 are the regression coefficients; and e is the regression residual. Therefore, the mean value (expected value) of ln*EDP* given a specified IM value (IM=*im*) can be calculated as:

$$E[\ln EDP | IM = im] = a_0 + a_1 \ln im \tag{10}$$

Assuming a constant variance for e for all the IM values, and Gaussian distribution for ln*EDP*|IM, the conditional probability of exceeding an *EDP* level y given IM=*im* can be obtained as:

$$G_{EDP|IM}(y|im)=1-\Phi\left(\frac{\ln y-(a_0+a_1 \ln im)}{\sqrt{Var[e]}}\right) \quad (11)$$

where $G_{EDP|IM}(y|im)$ is the complementary cumulative distribution function (CCDF) of *EDP*|IM; Φ() is the cumulative distribution function (CDF) of standard Gaussian distribution; and Var[e] is variance of *e* [2]. Figure 3 shows an example for cloud data, i.e., MIDR versus PGA for the 6-story structure (with h=0.003). In this figure, STD represents standard deviation of *e*, i.e., $\sqrt{Var[e]}$.

5. Efficiency of the IMs

The ability of an IM to anticipate the structural response with low dispersion is called efficiency. The efficiency of scalar IMs for the prediction of MIDR can be evaluated through applying the conditional standard deviation of lnMIDR, $\sigma_{lnMIDR|IM}$. Using an efficient IM reduces $\sigma_{lnMIDR|IM}$, and consequently, increases the reliability of the seismic performance assessments of the structures.

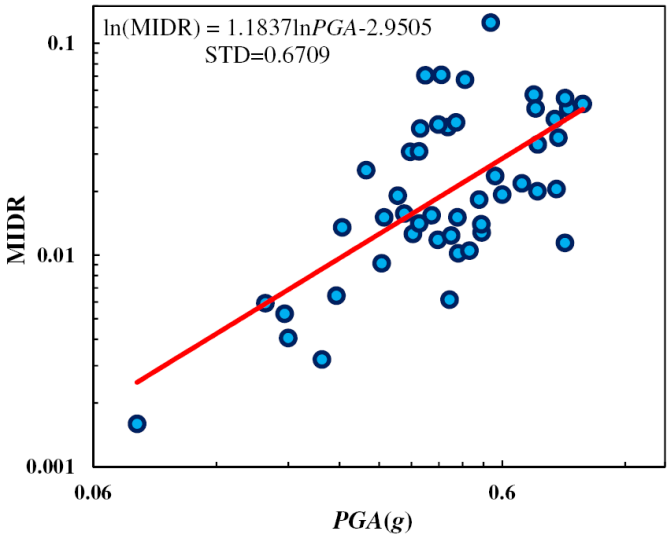

Fig. 3. A cloud of *EDP*|IM data (MIDR as *EDP* and PGA as IM).

Having $\sigma_{lnMIDR|IM}$ obtained by applying a scalar IM, the standard error (SE) [38] is defined as:

$$SE=\frac{\sigma_{lnMIDR}}{\sqrt{n_s}} \quad (12)$$

where n_s is the number of seismic response analyses. Based on Equation 12, it can be inferred that with the same number of analyses, the use of a more efficient IM decreases the SE value. Thus, for reducing the number of analyses and increasing the reliability of structural seismic response assessments, efficiency is one of the desirable features of an optimal IM.

In order to choose the most efficient IM for the prediction of MIDR demand, the values of $\sigma_{lnMIDR|IM}$ obtained using different IMs should be compared. The IM that is able to predict the structural response (i.e., MIDR) with a lower dispersion can be selected as a more efficient IM. Figure 4 illustrated the comparison between the efficiency of four scalar IMs for predicting MIDR demand on the 3-story structure (with h=0.003). As shown in this figure, using Sa_{avg} leads to the lowest dispersion (i.e., $\sigma_{lnMIDR|IM}$ =0.4304),

and therefore, it is more efficient than the other IMs.

Table 3 exhibits the results of investigating the efficiency of the IMs for predicting MIDR demand on the structures considered (with two different strain hardening ratios). As it is evident in this table, $IM_{M(\lambda=0.33)}$, IM_C, Sa_{avg} and $IM_{M(\lambda=0.5)}$ are the most efficient IMs for predicting MIDR demand on the 3-story structure (as a low-rise structure). It is also revealed that *PGV* among the traditional IMs, and $IM_{M(\lambda=0.33)}$, Sa_{avgM}, I_B and $IM_{M(\lambda=0.5)}$ among the advanced IMs can be chosen as the most efficient IMs for predicting MIDR demand on the 6- and 9-story structures (as mid-rise structures). In fact, $Sa(T_1)$ as the most prevalent scalar IM cannot efficiently predict MIDR demand on the low- to mid-rise BRB frames under near-fault ground motions, when compared with some of the IMs. As mentioned, above, the effect of strain hardening ratio on the efficiency of the IMs was also inspected. According to Table 3, it can be seen that by increasing the strain hardening ratio decreases the dispersion of the structural response prediction, whereas the order of the efficiency of the IMs does not changed.

Table 3. Results of testing the efficiency of the IMs (i.e., $\sigma_{\ln MIDR|IM}$) for predicting MIDR demand on the structures considered.

IM	Structure					
	3-story		6-story		9-story	
	h=0.003	h=0.02	h=0.003	h=0.02	h=0.003	h=0.02
PGA	0.6168	0.5563	0.6709	0.5667	0.7865	0.6948
PGV	0.6351	0.5767	0.4588	0.4207	0.4372	0.3827
PGD	0.8727	0.8003	0.7327	0.6645	0.6537	0.5846
$Sa(T_1)$	0.5927	0.5258	0.4794	0.4111	0.5360	0.4667
AI	0.6048	0.5548	0.6130	0.5243	0.6800	0.6102
CAV	0.7522	0.6942	0.6958	0.6115	0.6758	0.6146
I_{Np}	0.4627	0.4073	0.4456	0.3857	0.4944	0.4335
Sa_{avg}	0.4304	0.3862	0.4530	0.4009	0.4833	0.4363
Sa_{avgM}	0.4863	0.4339	0.4190	0.3395	0.4424	0.3772
IM_C	0.4262	0.3784	0.4571	0.4057	0.5141	0.4570
$IM_{M(\lambda=0.5)}$	0.4483	0.4003	0.4299	0.3831	0.4549	0.4182
$IM_{M(\lambda=0.33)}$	0.4085	0.3581	0.3823	0.3260	0.4466	0.3876
I_B	0.4800	0.4251	0.4290	0.3633	0.4631	0.3992

It is note-worthy to mention that the efficiency of an IM is gauged by the obtained dispersion of the structural capacity or response prediction using that IM. In addition, the severity of the non-linearity of the responses affects this dispersion. For example, Haselton and Deierlein [39] persuaded that the dispersion of collapse capacity of reinforced concrete special moment resisting frames (RC SMRFs) obtained based on $Sa(T_1)$ is approximately equal to 0.40. Yakhchalian and Ghodrati [6] manifested that under non-pulse-like ground motions the dispersion of MIDR demand on RC SMRFs obtained based on different IMs can vary between 0.20 and 0.55, depending on the structural height and the severity of the non-linearity of the responses. In the present study, as a result of using the near-fault records that are more severe than far-fault records, the obtained dispersions based on different IMs vary between 0.32 and 0.87.

Knowing that an optimal IM should also be sufficient, the sufficiency of the considered IMs is explored in the next section.

6. Sufficiency of the IMs

6.1. Sufficiency with respect to *M* and *R*

The sufficiency of a scalar IM for predicting the structural response means that the distribution of the structural response obtained based on the IM is independent of ground motion characteristics, such as earthquake magnitude (*M*), source-to-site distance (*R*), and in near-fault ground motions, pulse period (T_p) [3,7,17,21,23]. Since a finite number of analyses are used in order to obtain the distribution of the structural response, sufficiency is one of the main features of an optimal IM. In fact, if the obtained distribution is dependent on the *M*, *R* and T_p values of the ground motion records used, then, the distribution will be biased if the distribution of the *M*, *R* and T_p of the ground motion records applied in the structural response analyses is not the same as that of the ground motions that will occur at the site in the future [3,4]. Using a sufficient IM can decouple the seismic hazard and structural response analyses.

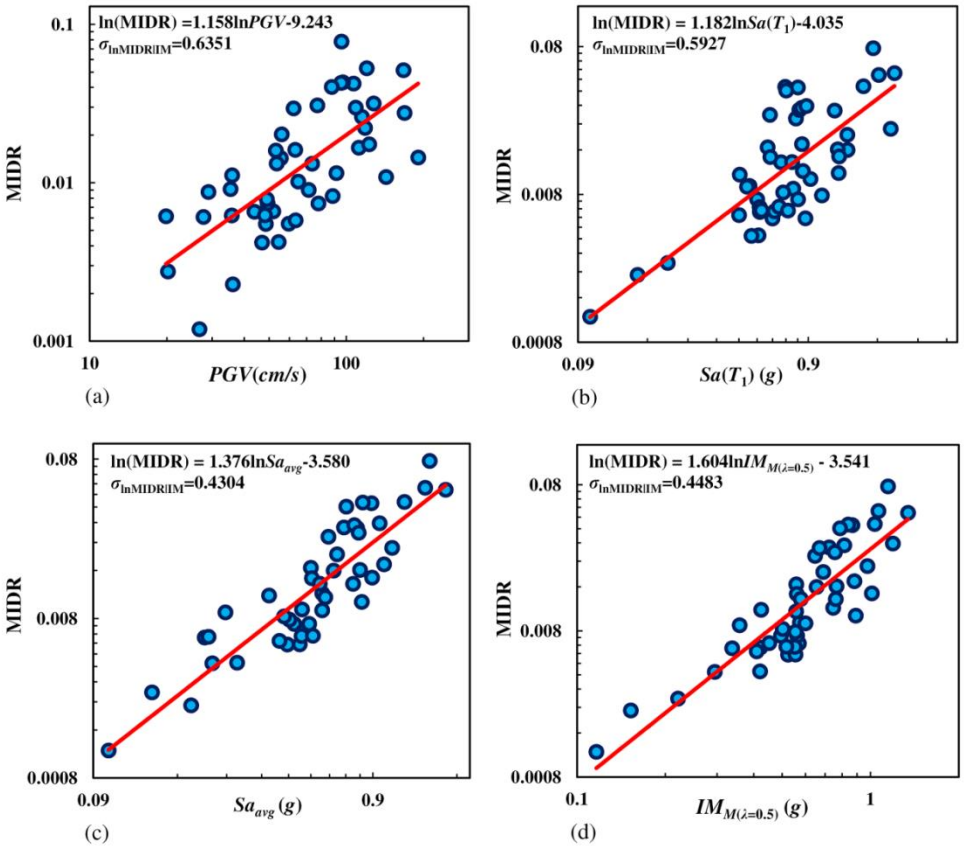

Fig. 4. Comparison of the efficiency of some scalar IMs for predicting MIDR demand on the 3-story structure: (a) *PGV*; (b) $Sa(T_1)$; (c) Sa_{avg}; (d) $IM_{M(\lambda=0.5)}$.

In order to inquire the sufficiency of the IMs with respect to *M* and *R* for predicting MIDR, linear regression can be used between the regression residuals obtained from Equation 9 and these ground motion characteristics as:

$$E[e]=b_0+b_1 x \quad (13)$$

where $E[e]$ is the expected value of e; b_0 and b_1 are the estimated coefficients of the linear regression; and x is M or the natural logarithm of R (ln$R$). Because the linear regression is based on a finite number of observations, testing the statistical significance of b_1 is essential. Therefore, assuming a student's-t distribution for b_1, the F-test can be applied to test the statistical significance of b_1 [40]. Generally, a p-value of less than 0.05 obtained from the F-test proves that b_1 is statistically significant, which means the insufficiency of the IM, applied in order to obtain the structural response distribution, with respect to x [3,4].

Figure 5 displays the results of testing the sufficiency of four IMs with respect to M for predicting MIDR demand on the 3-story structure (with h=0.003). In this figure, Res represents the regression residual obtained from Equation 9. As demonstrated in this figure, *PGV* cannot predict MIDR demand on the 3-story structure independent of M, because the obtained p-value is less than 0.05. In other words, *PGV* is insufficient with respect to M for predicting MIDR demand on the 3-story structure.

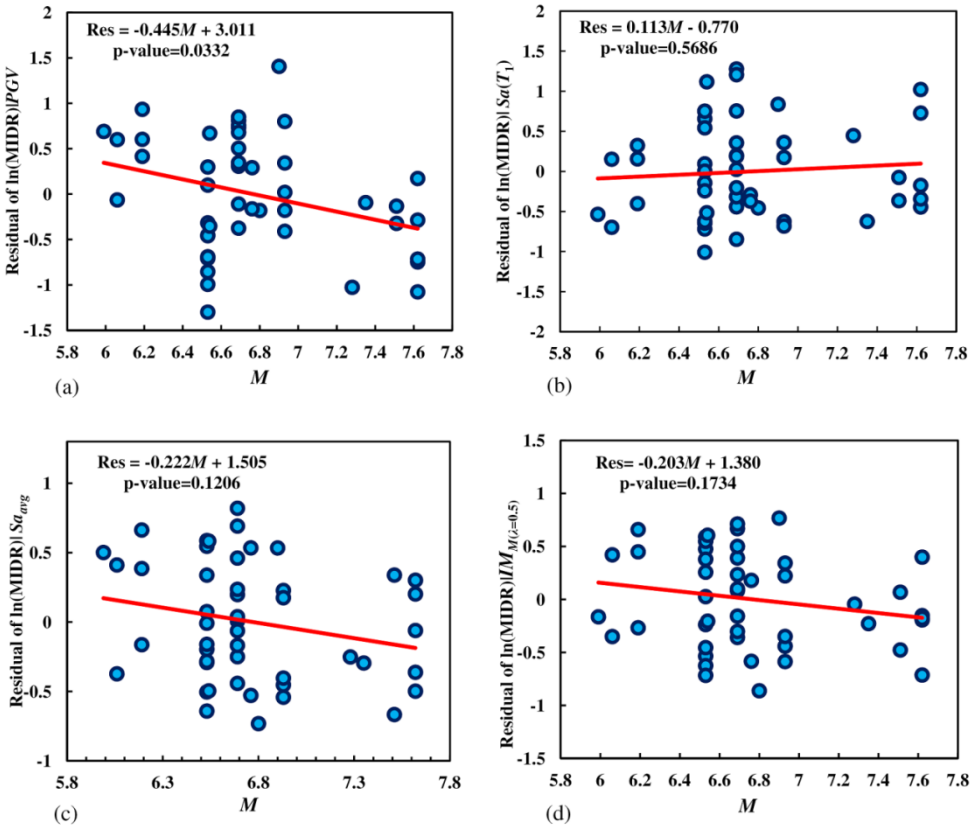

Fig. 5. Testing the sufficiency of four IMs with respect to M for predicting MIDR demand on the 3-story structure: (a) *PGV*, (b) $Sa(T_1)$, (c) Sa_{avg}, and (d) $IM_{M(\lambda=0.5)}$.

Table 4 the results of testing the sufficiency of the IMs with respect to M for predicting MIDR demand on the structures considered. It can be seen that all the IMs are sufficient with respect to M for predicting MIDR demand on the structures considered, except *PGV*, *AI*, and *CAV* that are insufficient (i.e., p-values<0.05) for predicting MIDR demand on the 3-story structure as a low-rise structure.

Figure 6 illustrates the results of testing the sufficiency of four IMs with respect to R for

predicting MIDR demand on the 3-story structure (with h=0.003). As shown in this figure, *PGV* is sufficient with respect to *R* for predicting MIDR demand on the 3-story structure (i.e., p-value>0.05), whereas the other IMs are not.

Table 4. Results of testing the sufficiency of the IMs with respect to *M* for predicting MIDR demand on the structures considered.

IM	Structure					
	3-story		6-story		9-story	
	h=0.003	h=0.02	h=0.003	h=0.02	h=0.003	h=0.02
PGA	0.7449	0.6193	0.0817	0.1322	0.0676	0.0535
PGV	0.0332	0.0200	0.4504	0.3107	0.9445	0.6722
PGD	0.3871	0.3556	0.3605	0.3636	0.2195	0.1719
$Sa(T_1)$	0.5686	0.6727	0.2906	0.4871	0.6270	0.7037
AI	0.0176	0.0114	0.9081	0.6477	0.7433	0.6605
CAV	0.0134	0.0117	0.2396	0.1582	0.2367	0.3177
I_{Np}	0.7905	0.9554	0.6136	0.9101	0.9385	0.9245
Sa_{avg}	0.1206	0.0668	0.7253	0.4786	0.4122	0.3267
Sa_{avgM}	0.5953	0.4481	0.4824	0.7982	0.1364	0.3001
IM_C	0.3226	0.2044	0.9862	0.7119	0.6443	0.5492
$IM_{M(\lambda=0.5)}$	0.1734	0.1015	0.3875	0.2213	0.1959	0.1458
$IM_{M(\lambda=0.33)}$	0.8601	0.9468	0.8178	0.4711	0.7431	0.5296
I_B	0.9278	0.9054	0.5135	0.8135	0.7061	0.9012

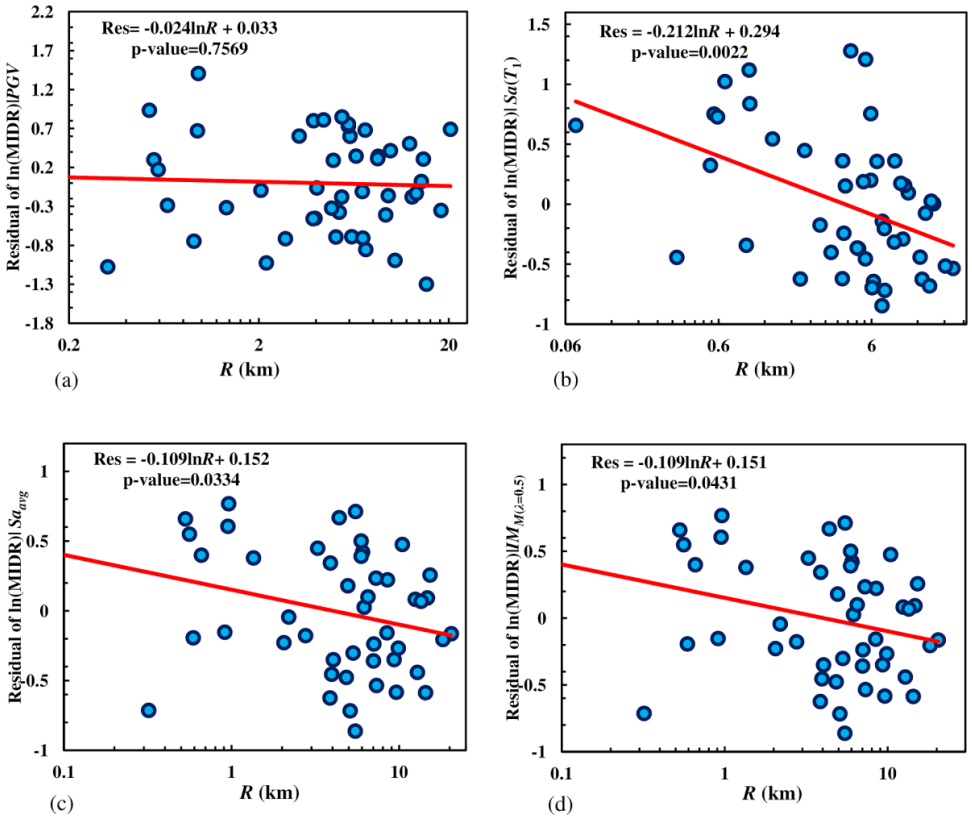

Fig. 6. Testing the sufficiency of four IMs with respect to *R* for predicting MIDR demand on the 3-story structure: (a) *PGV*, (b) $Sa(T_1)$, (c) Sa_{avg} and (d) $IM_{M(\lambda=0.5)}$

Table 5 shows the results of testing the sufficiency of the IMs with respect to *R* for predicting MIDR demand on the structures considered. It can be seen that only *PGV* can predict MIDR demand on the three structures independently of *R*. It is note-worthy to mention that *PGV* does not have a higher efficiency for predicting MIDR demand on the 3-story structure, in comparison with the other IMs, whereas it has an acceptable efficiency for the 6- and 9-story structures. It can therefore be inferred that most of the IMs (including advanced scalar IMs) cannot predict MIDR demand on the structures independently from *R*, under near-fault pulse-like ground motions.

Table 5. Results of testing the sufficiency of the IMs with respect to *R* for predicting MIDR demand on the structures considered.

IM	Structure					
	3-story		6-story		9-story	
	h=0.003	h=0.02	h=0.003	h=0.02	h=0.003	h=0.02
PGA	0.0089	0.0135	0.0005	0.0014	0.0005	0.0001
PGV	0.7569	0.8808	0.7629	0.9915	0.4949	0.4858
PGD	0.0131	0.0158	0.0280	0.0414	0.0176	0.0214
$Sa(T_1)$	0.0022	0.0032	0.0010	0.0044	0.0024	0.0010
AI	0.0728	0.0988	0.0061	0.0167	0.0045	0.0015
CAV	0.0414	0.0518	0.0070	0.0164	0.0045	0.0021
I_{Np}	0.0059	0.0094	0.0031	0.0126	0.0090	0.0052
Sa_{avg}	0.0334	0.0540	0.0672	0.1606	0.0652	0.0496
Sa_{avgM}	0.0122	0.0195	0.0339	0.0997	0.2133	0.1995
IM_C	0.0191	0.0314	0.0238	0.0685	0.0248	0.0164
$IM_{M(\lambda=0.5)}$	0.0431	0.0673	0.0430	0.1171	0.0522	0.0467
$IM_{M(\lambda=0.33)}$	0.0112	0.0183	0.0105	0.0414	0.0291	0.0216
I_B	0.0042	0.0068	0.0026	0.0107	0.0123	0.0075

6.2. Sufficiency with respect to T_p

To investigate the sufficiency of the IMs with respect to T_p, moving average curve can be applied [41]. The potential bias due to T_p (B_{Tp}), in structural response prediction, can be expressed by the total area between the moving average curve and the zero residual line. In fact, this area is a proxy for the effect of T_p that is unaccounted for by the IM. Therefore, an IM is more sufficient with respect to T_p than other IMs, when the B_{Tp} value obtained applying the IM is lower than those of the other ones.

Figure 7 illustrates the results of investigating the sufficiency of four IMs with respect to T_p for predicting MIDR demand on the 3-story structure (with h=0.003). As demonstrated in this figure, applying $IM_{M(\lambda=0.5)}$ leads to the lowest area between the moving average curve and the zero residual line (i.e., B_{Tp}=area=1.811), and therefore, $IM_{M(\lambda=0.5)}$ has a higher sufficiency with respect to T_p, in comparison with the other IMs.

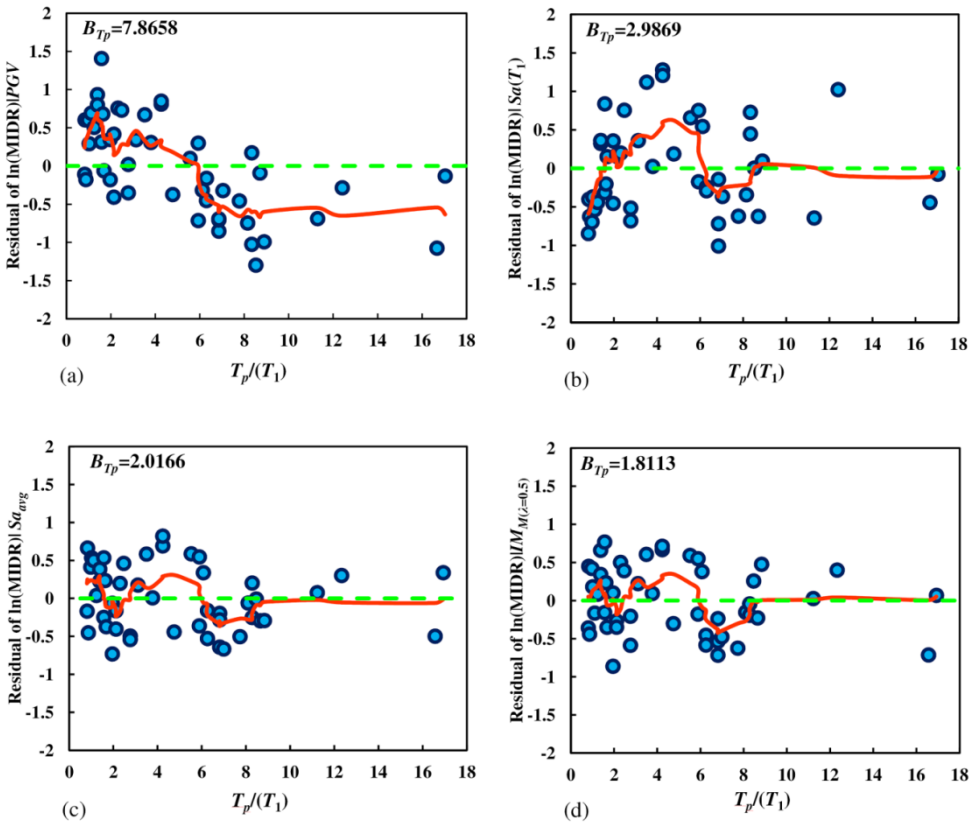

Fig. 7. Testing the sufficiency of four IMs with respect to T_p for predicting MIDR demand on the 3- story structure: (a) *PGV*, (b) $Sa(T_1)$, (c) Sa_{avg}, and (d) $IM_{M(\lambda=0.5)}$.

Table 6 presents the results of testing the sufficiency of the IMs with respect to T_p for predicting MIDR demand on the structures considered. As it is evident, *PGD* has the lowest sufficiency with respect to T_p for predicting MIDR demand on the structures, in comparison with the other IMs. In addition, none of the IMs has the highest sufficiency with respect to T_p for the three structures considering the two strain hardening ratios. It can be also observed that by increasing the height of structure, the sufficiency of the conventional IMs (i.e., *PGA*, *PGV*, *PGD*, and $Sa(T_1)$) and cumulative-based IMs (*AI* and *CAV*) with respect to T_p for predicting MIDR demand on the structures, increases. It should be mentioned that most of the advanced IMs are more sufficient than the conventional and cumulative-based IMs. In the case of the 3-story structure (as a low-rise structure), $IM_{M(\lambda=0.5)}$ and Sa_{avg} can be selected as the most sufficient IMs with respect to T_p for predicting MIDR demand. For the 6- and 9-story structures (as mid-rise structures), $Sa(T_1)$ and *PGV* are respectively the most sufficient IMs with respect to T_p, among the conventional and cumulative-based IMs. It is also shown that $IM_{M(\lambda=0.33)}$, I_{Np} and I_B can be selected as the most sufficient IMs with respect to T_p for predicting MIDR demand on the 6- and 9-story structures, considering the two strain hardening ratios.

Table 6. Results of testing the sufficiency of the IMs with respect to T_p for predicting MIDR demand on the structures considered.

IM	Structure					
	3-story		6-story		9-story	
	h=0.003	h=0.02	h=0.003	h=0.02	h=0.003	h=0.02
PGA	3.2727	3.2342	1.9984	1.4548	1.3834	1.3840
PGV	7.8658	7.4823	1.8087	1.9850	0.5415	0.6775
PGD	10.1338	9.4700	4.3174	4.0392	2.7456	2.4348
$Sa(T_1)$	2.9869	2.7756	1.1414	0.7147	0.7137	0.5770
AI	5.0306	4.9072	1.2425	1.0569	1.0097	0.9884
CAV	8.2008	7.7938	2.1123	2.2077	1.2030	0.9282
I_{Np}	2.3034	1.9998	0.7128	0.5713	0.6261	0.4592
Sa_{avg}	2.0166	2.0972	0.7503	1.0473	0.9209	0.8665
Sa_{avgM}	2.3158	1.9869	1.1640	0.7131	1.1911	0.7754
IM_C	2.0893	2.1581	0.7743	1.0411	0.7987	0.6957
$IM_{M(\lambda=0.5)}$	1.8113	1.7054	0.8071	1.1059	0.9560	0.9708
$IM_{M(\lambda=0.33)}$	2.8513	2.4702	0.4406	0.6330	0.5906	0.5137
I_B	2.3116	2.0255	1.0220	0.5612	0.5481	0.3426

7. Selection of optimal IMs

Knowing that an optimal IM requires to be efficient and sufficient to accurately anticipate the seismic response of structures, in the previous sections, efficiency and sufficiency of the IMs deliberated were investigated. As the results show, it is unlikely possible to find an IM that is the most efficient and also sufficient for the three structures. Consequently, the results are divided into two parts belonging to low- and mid-rise structures.

In the case of the 3-story structure (as a low-rise structure), it was depicted that $IM_{M(\lambda=0.33)}$, IM_C, Sa_{avg} and $IM_{M(\lambda=0.5)}$ are the most efficient IMs for predicting MIDR. The results of testing the sufficiency of the IMs showed that these IMs are sufficient with respect to *M*. In addition, it was also shown that $IM_{M(\lambda=0.5)}$ and Sa_{avg} can be selected as the most sufficient IMs with respect to T_p. Investigating the sufficiency of the IMs showed that *PGV* and *AI* are the only sufficient IMs with respect to *R*, considering both the strain hardening ratios. Put it differently, due to their lower efficiency and sufficiency with respect to T_p, *PGV* and *AI* cannot be selected as optimal IMs. Therefore, $IM_{M(\lambda=0.5)}$ and Sa_{avg} due to their higher efficiency and sufficiency with respect to T_p, were selected as optimal IMs for predicting MIDR demand on the low-rise steel BRB frames under near-fault ground motions. As a result of the insufficiency of $IM_{M(\lambda=0.5)}$ and Sa_{avg} with respect to *R*, to have a reliable and realistic prediction of MIDR demand on low-rise steel BRB frames by using these IMs, ground motion record selection for conducting non-linear dynamic analyses is require to be performed pondering *R* to be compatible with the results of probabilistic seismic hazard analysis.

In the case of the 6- and 9-story structures (as mid-rise structures), it was shown that *PGV* among the traditional and cumulative-based IMs, and $IM_{M(\lambda=0.33)}$, Sa_{avgM}, I_B and $IM_{M(\lambda=0.5)}$ among the advanced IMs can be selected as the more efficient IMs than the other ones. Investigating the sufficiency of the IMs for the mid-rise structures demonstrated that all

the IMs are sufficient with respect to *M*. In addition, only *PGV* is sufficient with respect to *R*. It is note-worthy to mention that *PGV* has an acceptable efficiency for the mid-rise structures. Investigating the sufficiency of the IMs with respect to T_p displayed that $Sa(T_1)$ and *PGV* are the most sufficient IMs with respect to T_p among the traditional and cumulative-based IMs. In the case of the advanced IMs, it was also exhibited that $IM_{M(\lambda=0.33)}$, I_{Np} and I_B can be selected as the most sufficient IMs with respect to T_p, considering both the strain hardening ratios. Therefore, *PGV* can be selected as an optimal IM that has acceptable efficiency and sufficiency with respect to *M*, *R*, and T_p for predicting MIDR demand on the mid-rise steel BRB frames under near-fault ground motions. It should be noted that, the advanced IM $IM_{M(\lambda=0.33)}$ due to its acceptable efficiency and sufficiency with respect to *M* and T_p can also be selected as an optimal IM for predicting MIDR demand on the mid-rise steel BRB frames under near-fault ground motions. We also should mention that, due to the insufficiency of $IM_{M(\lambda=0.33)}$ with respect to *R*, to have a reliable prediction of MIDR demand by using $IM_{M(\lambda=0.33)}$, ground motion record selection needs to be performed considering *R* to be compatible with the results of probabilistic seismic hazard analysis.

As mentioned previously, applying optimal IMs makes the structural seismic response assessments more reliable. For example, in the case of the 3-story structure (with a strain hardening ratio of 0.003), using $Sa(T_1)$ as a traditional IM and $IM_{M(\lambda=0.5)}$ as an optimal IM results in dispersions of 0.593 and 0.409 in the prediction of MIDR demand, respectively. Regarding Equation 12, using $IM_{M(\lambda=0.5)}$ instead of $Sa(T_1)$ can lead to a reduction of 31% in SE. Furthermore, the acceptable sufficiency of $IM_{M(\lambda=0.5)}$ with respect to *M* and T_p makes the assessments independent of *M* and T_p of the ground motion records used.

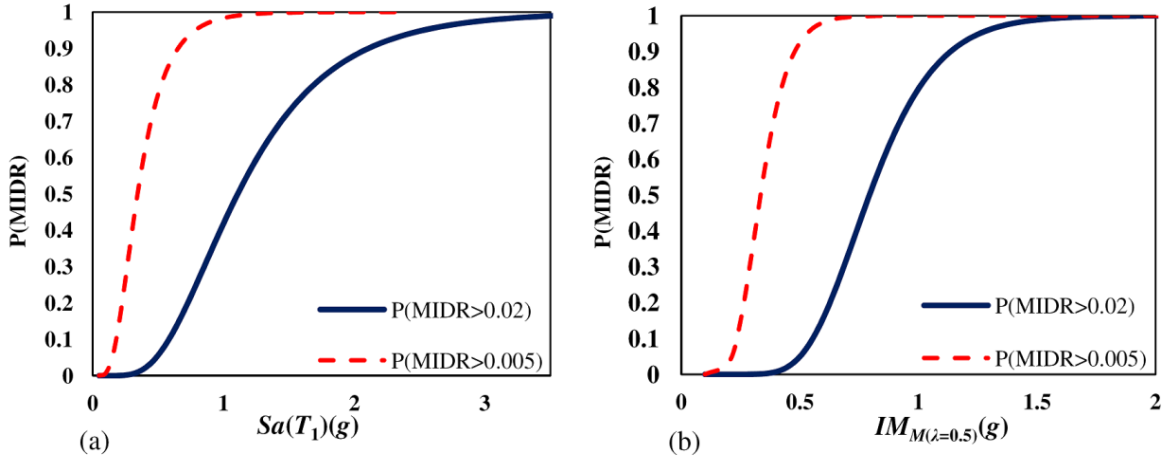

Fig. 8. Fragility curves obtained by $Sa(T_1)$ and $IM_{M(\lambda=0.5)}$ for the 3-story structure: (a) $Sa(T_1)$, (b) $IM_{M(\lambda=0.5)}$.

One of the most prevalent applications of IMs in the PBEE is the calculation of the fragility curve for a structure, which proves the probability of exceedance from a specific value of an EDP, or a considered limit state (e.g., see [42–44]). Figure 8 portrayed the fragility curves obtained by $Sa(T_1)$ and $IM_{M(\lambda=0.5)}$, using Equation 11, for the 3-story structure (with h=0.003). Due to the higher efficiency and sufficiency of $IM_{M(\lambda=0.5)}$ than $Sa(T_1)$, it can be concluded that the fragility curves obtained by $IM_{M(\lambda=0.5)}$ are more reliable than those obtained by $Sa(T_1)$.

It is worth mentioning that, this study focused on the investigation of the efficiency and sufficiency of the IMs for predicting MIDR demand on the steel BRB frames under near-fault ground motions. On that account, an inquiry for selecting optimal IMs for collapse capacity prediction of the considered structures can be conducted as a future work. Moreover, the results of this study were obtained in consonance with an investigation on three regular steel BRB frames. Thus, the efficiency and sufficiency of the IMs may significantly vary if irregular structures are considered.

8. Conclusions

In this study, the efficiency and sufficiency of 13 IMs including traditional IMs, cumulative-based IMs (i.e., AI and CAV), and advanced IMs for predicting MIDR on the low- to mid-rise steel BRB frames under near-fault ground motions (having forward directivity) were investigated. To this end, three structures including 3-, 6- and 9-story steel BRB frames considering two strain hardening ratios for steel material model in each structure were deliberated. The results proves that $Sa(T_1)$ as the most prevalent scalar IM cannot efficiently and sufficiently predict MIDR demand on the low- to mid-rise steel BRB frames under near-fault ground motions, when compared with some of the IMs considered. It was also demonstrated that, most of the IMs (including advanced scalar IMs) are insufficient with respect to R for predicting MIDR demand on the structures under near-fault pulse-like ground motions. In addition, investigating the effect of strain hardening ratio on the efficiency and sufficiency of the IMs revealed that increasing the strain hardening ratio decreases the dispersion in the structural response prediction (i.e., increases the efficiency), whereas the order of the efficiency of the IMs does not change. However, the order of the sufficiency of the IMs can alternate when the strain hardening ratio varies. it is note-worthy to mention that, most of the advanced IMs are more sufficient with respect to T_p than the conventional and cumulative-based IMs.

The results revealed that it is unlikely possible to find an IM that is the most efficient and also sufficient for the three structures. On that account, the conclusions are divided into two parts belonging to low- and mid-rise structures. In the case of the 3-story structure (as a low-rise structure), due to the higher efficiency and sufficiency of $IM_{M(\lambda=0.5)}$ and Sa_{avg} with respect to T_p, they were selected as optimal IMs for predicting MIDR demand on the low-rise steel BRB frames under near-fault ground motions. It should be noted that, as a result of the insufficiency of $IM_{M(\lambda=0.5)}$ and Sa_{avg} with respect to R, to have a reliable and realistic prediction of MIDR demand on low-rise steel BRB frames by using these IMs, ground motion selection for conducting non-linear dynamic analyses require to be performed contemplating R to be compatible with the results of probabilistic seismic hazard analysis. In the case of the 6- and 9-story structures (as mid-rise structures), PGV and $IM_{M(\lambda=0.33)}$ were selected as optimal IMs for predicting MIDR demand on the mid-rise steel BRB frames under near-fault ground motions. As a result of the insufficiency of $IM_{M(\lambda=0.33)}$ with respect to R, to have a reliable prediction of MIDR demand on the mid-rise steel BRB frames by using $IM_{M(\lambda=0.33)}$, ground motion selection is required to be performed considering R to be compatible with the results of probabilistic seismic hazard analysis.

REFERENCES

[1] Moehle, J., Deierlein, G. G. (2004). "A framework methodology for performance-based earthquake engineering", In: Proceedings of the 13th World Conference on Earthquake Engineering, Vancouver, BC, Canada.

[2] Baker, J. W. (2005). "Vector-valued ground motion intensity measures for probabilistic seismic demand analysis", Dissertation, Department of Civil and Environmental Engineering, Stanford University.

[3] Bradley, B. A., Dhakal, R. P., MacRae G. A., Cubrinovski, M. (2010). "Prediction of Spatially Distributed Seismic Demands in Specific Structures: Ground Motion and Structural Response", Earthquake Engineering and Structural Dynamics, Vol. 39, Issue 5, pp. 501–520. doi: 10.1002/eqe.954.

[4] Yakhchalian, M., Nicknam, A., Ghodrati Amiri, G. (2015). "Optimal vector-valued intensity measure for seismic collapse assessment of structures", Earthquake Engineering and Engineering Vibration, Vol. 14, Issue 1, pp. 37–54. doi: 10.1007/s11803-015-0005-6.

[5] Kiani, J., Pezeshk, S. (2017). "Sensitivity analysis of the seismic demands of RC moment resisting frames to different aspects of ground motions", Earthquake Engineering and Structural Dynamics, Vol. 46, Issue 15, pp. 2739–2755. doi: 10.1002/eqe.2928.

[6] Yakhchalian, M., Ghodrati Amiri, G. (2018). "A vector intensity measure to reliably predict maximum drift in low- to mid-rise buildings", Proceedings of the Institution of Civil Engineers-Structures and Buildings, pp. 1–13. doi: 10.1680/jstbu.17.00040.

[7] Tothong, P., Cornell, C. A. (2008). "Structural performance assessment under near-source pulse-like ground motions using advanced ground motion intensity measures", Earthquake Engineering & Structural Dynamics, Vol. 37, Issue 7, pp. 1013–1037.

[8] Yakhchalian, M., Nicknam, A., Ghodrati Amiri, G. (2014). "Proposing an optimal integral-based intensity measure for seismic collapse capacity assessment of structures under pulse-like near-fault ground motions", Journal of Vibroengineering, Vol. 16, Issue 3, pp. 1360–1375.

[9] Kalkan, E., Kunnath, S. K. (2006). "Effects of fling step and forward directivity on seismic response of buildings", Earthquake spectra, Vol. 22, Issue 2, pp. 367–390.

[10] Memarpour, M. M., Ghodrati Amiri, G., Razeghi, H., Akbarzadeh, M., Davoudi, A. T. (2016). "Characteristics of horizontal and vertical near-field ground motions and investigation of their effects on the dynamic response of bridges", Journal of Rehabilitation in Civil Engineering, Vol. 4, Issue 2, pp. 1–24.

[11] Champion, C., Liel, A. (2012). "The effect of near-fault directivity on building seismic collapse risk", Earthquake Engineering and Structural Dynamics, Vol. 41, Issue 10, pp. 1391–1409.

[12] Rai, D. C., Goel, S. C. (2003). "Seismic evaluation and upgrading of chevron braced frames", Journal of Constructional Steel Research, Vol. 59, Issue 8, pp. 971–994.

[13] Asgarian, B., Shokrgozar, H. R. (2009). "BRBF response modification factor", Journal of constructional steel research, Vol. 65, Issue 2, pp. 290-298. doi: 10.1016/j.jcsr.2008.08.002.

[14] Bosco, M., Edoardo, M. M. (2013). "Design method and behavior factor for steel frames with buckling restrained braces", Earthquake Engineering and Structural Dynamics, Vol. 42, Issue 8, pp. 1243–1263.

[15] Abdollahzadeh, G., Farzi-Bashir, H., Banihashemi, M. (2014). "Seismic retrofitting of steel frames with buckling restrained and ordinary concentrically bracing systems with various strain hardening and slenderness ratios", Journal of Rehabilitation in Civil Engineering, Vol. 2, Issue 2, pp. 20–31. doi: 10.22075/jrce.2014.205.

[16] Hosseinzadeh, S., Mohebi, B., (2016). "Seismic evaluation of all-steel buckling restrained braces using finite element analysis", Journal of Constructional Steel Research, Vol. 119, pp. 76–84. doi:10.1016/j.jcsr.2015.12.014.

[17] Jamshidiha, H. R., Yakhchalian, M., Mohebi, B. (2018). "Advanced scalar intensity measures for collapse capacity prediction of steel moment resisting frames with fluid viscous dampers", Soil Dynamics and Earthquake Engineering, Vol. 109, pp. 102–118. doi: 10.1016/j.soildyn.2018.01.009.

[18] Cordova, P. P., Deierlein, G. G., Mehanny, S. S., Cornell, C.A. (2000). "Development of a two-parameter seismic intensity measure and probabilistic assessment procedure", In the second US-Japan workshop on performance-based earthquake engineering methodology for reinforced concrete building structures, pp. 187–206.

[19] Mehanny, S. S. (2009). "A broad-range power-law form scalar-based seismic intensity measure", Engineering Structures, Vol. 31, Issue 7, pp. 1354–68. doi: 10.1016/j.engstruct.2007.07.009.

[20] Bojórquez, E., Iervolino, I. (2011). "Spectral shape proxies and non-linear structural response", Soil Dynamics and Earthquake Engineering, Vol. 31, Issue 7, pp. 996–1008. doi: 10.1016/j.soildyn.2011.03.006.

[21] Eads, L., Miranda, E., Lignos, D. G. (2015). "Average spectral acceleration as an intensity measure for collapse risk assessment", Earthquake Engineering and Structural Dynamics, Vol. 44, Issue 12, pp. 2057–73. doi: 10.1002/eqe.2575.

[22] Bojórquez, E., Chávez, R., Reyes-Salazar, A., Ruiz, S. E., Bojórquez, J. (2017). "A new ground motion intensity measure I_B", Soil Dynamics and Earthquake Engineering, Vol. 99, pp. 97–107. doi: 10.1016/j.soildyn.2017.05.011.

[23] Tothong, P., Luco, N. (2007). "Probabilistic seismic demand analysis using advanced ground motion intensity measures", Earthquake Engineering and Structural Dynamics, Vol. 36, Issue 13, pp. 1837–1860.

[24] Yakhchalian, M., Ghodrati Amiri, G., Nicknam, A. (2014). "A new proxy for ground motion selection in seismic collapse assessment of tall buildings", The Structural Design of Tall and Special Buildings, Vol. 23, Issue 17, pp. 1275–1293. doi: 10.1002/tal.1143.

[25] Yakhchalian, M., Ghodrati Amiri, G., Eghbali, M. (2017). "Reliable seismic collapse assessment of short-period structures using new proxies for ground motion record selection", Scientia Iranica, Vol. 24, Issue 5, pp. 2283–2293. doi: 10.24200/sci.2017.4162.

[26] Koopaee, M. E., Dhakal, R. P., MacRae, G. (2017). "Effect of ground motion selection methods on seismic collapse fragility of RC frame buildings", Earthquake Engineering and Structural Dynamics, Vol. 46, Issue 11, pp. 1875–1892. doi: 10.1002/eqe.2891.

[27] Arias, A. (1970). "A measure of earthquake intensity", In Seismic design for nuclear power plants, R. J. Hansen (ed.), The MIT Press, Cambridge, MA, pp. 438–483.

[28] Benjamin, J. R. (1988). "A criterion for determining exceedances of the operating basis earthquake", EPRI Report NP-5930, Electric Power Research Institute, Palo Alto.

[29] ASCE (American Society of Civil Engineers). (2010). ASCE 7-10 Minimum design loads for buildings and other structures, ASCE, Reston, VA, USA.

[30] AISC Committee. (2010). Specification for Structural Steel Buildings (ANSI/AISC 360-10), American Institute of Steel Construction, Chicago-Illinois.

[31] AISC Committee. (2010). Seismic provisions for structural steel buildings (AISC 341-10), American Institute of Steel Construction, Chicago-Illinois.

[32] Open System for Earthquake Engineering Simulation (OpenSees). (2013). Pacific Earthquake Engineering Research Center, University of California, Berkeley, http://opensees.berkeley.edu.

[33] Mazzoni, S., McKenna, F. H., Scott, M. L., Fenves, G. (2006). OpenSees command language manual.

[34] Guerrero, H., Ji, T., Teran-Gilmore, A., Escobar, J. A. (2016). "A method for preliminary seismic design and assessment of low-rise structures protected with Buckling-Restrained Braces", Engineering Structures, Vol. 123, pp.141–154. doi: 10.1016/j.engstruct.2016.05.015.

[35] Mahdavipour, M. A., Deylami, A. (2014). "Probabilistic assessment of strain hardening ratio effect on residual deformation demands of Buckling-Restrained Braced Frames", Engineering Structures, Vol. 81, pp. 302–308. doi: 10.1016/j.engstruct.2014.10.004.

[36] Uriz, P. (2008). "Toward earthquake-resistant design of concentrically braced steel-frame structures", Pacific Earthquake Engineering Research Center.

[37] Pacific Earthquake Engineering Research Center (PEER). (2013). PEER Next Generation Attenuation (NGA) Database. https://ngawest2.berkeley.edu

[38] Benjamin, J. R., Cornell, C. A. (1970). "Probability, statistic, and decision for civil engineers", New York: McGraw-Hill.

[39] Haselton, C. B., Deierlein, G. G. (2008). "Assessing Seismic Collapse Safety of Modern Reinforced Concrete Moment-frame Buildings", PEER Report 2007/08, Pacific Engineering Research Center, University of California, Berkeley, CA.

[40] ANG H-S, A., TANG, H. W. (1975). "Probability concepts in engineering planning and design", Vol. 1, Basic Principles.

[41] Baker, J. W., Cornell, C. A. (2008). "Vector-valued intensity measures for pulse-like near-fault ground motions", Engineering Structures, Vol. 30, Issue 4, pp. 1048–57. doi: 10.1016/j.engstruct.2007.07.009.

[42] Maleki, M., Ahmady Jazany, R., Ghobadi, M. S., (2018). "Probabilistic Seismic Assessment of SMFs with Drilled Flange Connections Subjected to Near-Field Ground Motions", International Journal of Steel Structures, pp. 1–17. doi: 10.1007/s13296-018-0112-0.

[43] Yahyaabadi, A. Tehranizadeh, M. (2011). "New scalar intensity measure for near-fault ground motions based on the optimal combination of spectral responses", Scientia Iranica, Vol. 18, Issue 6, pp. 1149–1158. doi: 10.1016/j.scient.2011.09.013.

[44] Yahyazadeh, A., Yakhchalian, M. (2018). "Probabilistic residual drift assessment of SMRFs with linear and nonlinear viscous dampers", Journal of Constructional Steel Research, Vol. 148, pp. 409–421. doi: 10.1016/j.jcsr.2018.05.031.